energies

MDPI

Article

Solar Farm Suitability Using Geographic Information System Fuzzy Sets and Analytic Hierarchy Processes: Case Study of Ulleung Island, Korea

Jangwon Suh * and Jeffrey R. S. Brownson

John & Willie Leone Department of Energy and Mineral Engineering, The Pennsylvania State University, University Park, PA 16802, USA; jrb52@psu.edu

* Correspondence: jangwonsuh@hanmail.net; Tel.: +1-814-883-9907

Academic Editor: Tapas Mallick

Received: 13 June 2016; Accepted: 10 August 2016; Published: 17 August 2016

Abstract: Solar farm suitability in remote areas will involve a multi-criteria evaluation (MCE) process, particularly well suited for the geographic information system (GIS) environment. Photovoltaic (PV) solar farm criteria were evaluated for an island-based case region having complex topographic and regulatory criteria, along with high demand for low-carbon local electricity production: Ulleung Island, Korea. Constraint variables that identified areas forbidden to PV farm development were consolidated into a single binary constraint layer (e.g., environmental regulation, ecological protection, future land use). Six factor variables were selected as influential on-site suitability within the geospatial database to seek out increased annual average power performance and reduced potential investment costs, forming new criteria layers for site suitability: solar irradiation, sunshine hours, average temperature in summer, proximity to transmission line, proximity to roads, and slope. Each factor variable was normalized via a fuzzy membership function (FMF) and parameter setting based on the local characteristics and criteria for a fixed axis PV system. Representative weighting of the relative importance for each factor variable was assigned via pairwise comparison completed by experts. A suitability index (*SI*) with six factor variables was derived using a weighted fuzzy summation method. Sensitivity analysis was conducted to assess four different *SI* based on the development scenarios (i.e., the combination of factors being considered). From the resulting map, three highly suitable regions were suggested and validated by comparison with satellite images to confirm the candidate sites for solar farm development. The GIS-MCE method proposed can also be applicable widely to other PV solar farm site selection projects with appropriate adaption for local variables.

Keywords: solar farm; suitability analysis; geographic information systems (GISs); multi-criteria evaluation (MCE); fuzzy sets; Ulleung Island

1. Introduction

In recent years, interest in sustainable energy supplies has been growing rapidly as world demand for energy is expected to increase rapidly in the coming decades [1]. As a result of recent international commitments to Conference of Parties 21 (COP21) in Paris, that energy must be supplied by low-carbon strategies [2]. For the past decade, the adoption of solar energy has expanded to local-scale off-grid islands in many countries [3–7], off-grid mining areas [8–10], as well as extensive inland areas for the generation of electricity with lower CO_2 emissions.

Korea, which is a peninsula, has more than 3000 islands of different sizes. Many of them do not have electrical power grid systems connected with the mainland, using diesel fuel and local engines to generate electricity at a point source. Diesel power generation is typical of island communities

globally, yet the cost of operation is exceedingly high compared to the mainland due to the high transportation cost of fossil fuels [11]. Additionally, a diesel fuel supply for power generation contributes substantially to regional carbon emissions and local environmental pollution including methane (CH_4), sulfur oxides (SO_2), nitrous oxide (N_2O), chlorofluorocarbons (CFCs), and volatile organic compounds (VOCs) [12,13]. To address this challenge in Korea, the national government has developed strategies for new sustainable renewable energy systems for the islands with objectives of low-carbon, localized electricity production [14,15]. Ulleung Island was chosen to be the first candidate to become a "green island," and is well known for its tourism industry [16]. As a consequence, the Korean government initiated the "Green Ulleung Island Design Project" to develop all possible clean renewable energy systems (e.g., photovoltaic (PV), solar heat, wind power, geothermal, biomass, and hydropower) including an energy storage system (ESS) for the island that will generate 100% of its electricity demand by 2030. In particular, a PV system was chosen by a preference survey of the residents, conducted by the Ministry of Knowledge Economy of Korea, to examine the question "Which renewable energy source is most suitable considering the environmental condition of the island and the economic feasibility and maintenance aspects of the system?" [15]. We have thus chosen to use the island context of Ulleung Island to explore a multi-criteria evaluation (MCE) process for PV solar farm suitability in a complex locale.

Here, we frame the specific term locale to refer to the contextual constraints in space/time with respect to the local solar resource, the local environmental conditions (also ecosystems), the local energy/resource costs, and the local policies. In essence, all solar project development is local, and specific knowledge of locale is essential for a rewarding project development process. Spatial and temporal constraint variables will restrict or reduce access to solar development. Local knowledge of social and environmental/ecosystems factors from locale can increase annual system performance and reduce long-term risks of system failures [11]. For the development of PV farms in a specific region such as a volcanic island hosting a robust tourism industry, suitability analysis is an indispensable process enabled by the geographic information system (GIS) environment. In this case, site selection analysis has been based on a wide range of information to seek to maximize the profitability for project developers, while minimizing risk by offering non-trivial solutions to two selective project design goals: (1) increasing average annual power performance; and (2) reducing balance of system (BoS) costs.

Table 1 summarizes prior investigations that explored suitability assessments and site selection analyses for PV systems, in particular those using a MCE method in a GIS environment. Two criteria are grouped from variables used in GIS-based solar farm site selection studies. One is "constraint variables" that restrict site selection, and the other is "factor variables" that enable selective project goals by assessing the suitability of the non-constraint areas by identifying values with high suitability for development of a solar farm. Associated variables for each criterion are listed as well. Variables with high counts suggest important variables or generally applicable variables, while variables with low counts suggest less important variables or location-specific variables.

Table 1. Summary of factor variables and constraint variables used in previous geographic information system (GIS)-based solar farm site selection studies.

Variables		EPA [17]	Carrión et al. [18]	Charabi and Gastli [19]	Uyan [20]	Sánchez-Lozano et al. [21]	Watson and Hudson [22]	Raw Count
Factor variables	Solar irradiation	X	X	X	-	X	X	5
	Diffuse irradiation	-	X	-	-	-	-	1
	Equivalent sun hours	-	X	-	-	-	-	1
	Average temperature	-	X	-	-	X	-	2
	Road access	X	X	X	X	X	X	6
	Grid connection [1]	X	X		X	X	X	5
	Slope	X	X	X	X	X	X	6
	Aspect (orientation)	-	X	-	-	X	X	3
	Minimum suitable areas	X	-	-	-	X	-	2
	Agrological capacity	-	-	-	-	X	-	1
Constraint variables	Urban areas	X	X	X	X	X	X	6
	Residential areas		X	X	X	X	X	5
	Wildlife designations [2]	X	X	-	X	X	X	5
	Hydrographic areas [3]	X	X	X	X	X	-	5
	Touristic sites [4]	-	-	X	X	X	X	4
	Landscape designations [5]	X	X	-	-	X	X	4
	Traffic areas	-	X	X	X	-	-	3
	Sand/dusk risk	-	-	X	-	-	-	1
	Land subsidence	X	-	-	-	-	-	1
	Soil erosion	X	-	-	-	-	-	1

[1] Substation, transmission line, power line; [2] Bird protection zone, paleontological sites; [3] River, dams, flood area, water courses, streams; [4] Historical areas, cultural heritage, archeological sites; [5] Visual impact, scenic sites.

Pohekar and Ramachandran [23] and Wang et al. [24] have reviewed a variety of methods of multi-criteria decision analysis (MCDA) used in sustainable energy planning such as site selection. Diverse techniques have been explored to assess site suitability, including the analytic hierarchy process (AHP) techniques [18,20,22], the fuzzy logic ordered weight averaging (FLOWA) model [19], the technique for order preference by similarity to an ideal solution (TOPSIS) [25], and elimination and choice translating reality (ELECTRE) method [21]. Most methods, including the FLOWA model, can employ only a monotonic linear standardization function or simple scoring technique which is most appropriate for national-scale assessment in initial stage of land planning. The fuzzy set method can provide a variety of membership functions suited for the characteristics of each factor variable related with PV suitability. Relatively little work has been developed for the fuzzy membership function (FMF, not fuzzy combinational operator or fuzzy logic) of assessing PV solar farm site suitability. The FMF, first developed by Zadeh [26], makes it possible to represent and process uncertain data or incomplete rules in the GIS environment and information described in a common language and for which no certainty degree can be determined [27]. The value of representing and processing uncertain data or incomplete rules in GIS for solar is particularly important, as region-scale scenarios rarely hold complete regional data sets with respect to solar project factors. Hence, the use of FMF was deemed appropriate for this regional-scale study.

In addition, factor variables can have different intensities of importance to the spatio-temporal evaluation process of PV project site suitability. The AHP technique is a commonly used weighted summation method in an MCE because of its precision and ease of use. Hence the AHP technique was applied in this study by weighting factor variables to generate a single PV suitability index (SI).

The objective of this research is to explore an MCE method via GIS-enabled FMF and AHPs for selecting highly suitable PV solar farm areas (e.g., high solar utility). The locale of the work is an island-based case with complex topographic and regulatory criteria, and with high demand for low-carbon local electricity production. This study comprises the following stages: (1) identify constraint variables that restrict site selection, along with factor variables that enable selective project goals; (2) assess PV *SI* relative to the scale and spatial extent of the study area using the MCE method incorporating FMF and AHP techniques; (3) conduct a sensitivity and validation study to obtain a reliable suitability layer to facilitate the decision-making process for the design of a green island.

2. Methodology

Figure 1 presents a flow chart showing a GIS-based PV solar farm site suitability analysis model designed based on the four-step procedure (definition of objectives, specification of criteria, establishment of the decision rule, and determination of the goal) in a general MCE [28–30]. The objective of this research was to find the most suitable sites that maximize the annual electricity production and minimize the potential investment costs. Investigations and data collection on the study area were conducted (Section 2.1). Numerous factor variables and constraint variables were selected (Sections 2.2 and 2.3), fuzzy sets and AHP technique were used to establish decision rules (Sections 2.4 and 2.5), and sensitivity analyses based on the development scenarios were conducted to compare the results and to obtain the final goal (Section 2.6). ArcMap 10.1 Software (ESRI, Redlands, CA, USA) was used for processing and analysis of the data since it can perform a large array of functions associated with GIS-based MCE. All data files used in this study were converted from vector file or set to raster with a resolution of 5 m in consideration of the extent of the study areas.

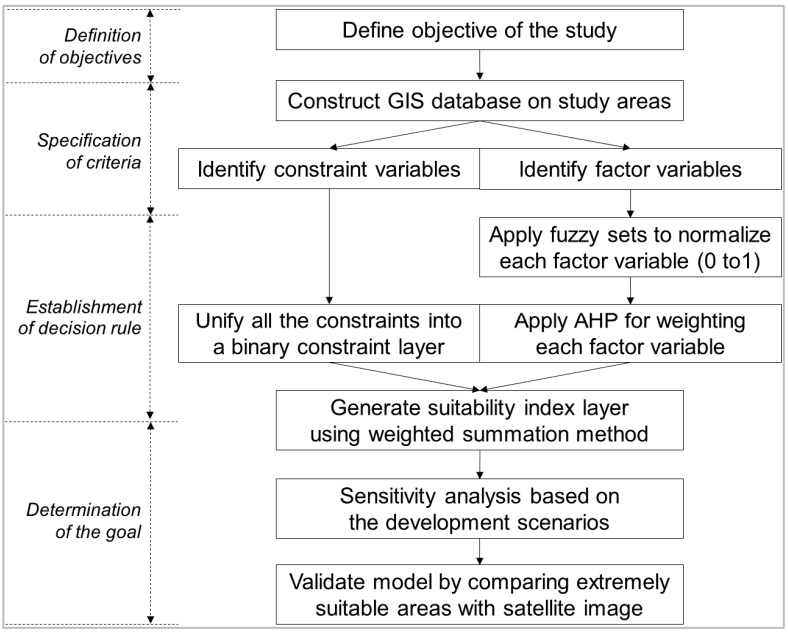

Figure 1. Flow chart of photovoltaic (PV) solar farm site suitability analysis model designed based on the four phases of multi-criteria evaluation (MCE) process in a GIS environment.

2.1. Study Area

As seen in Figure 2a, Ulleung Island is a roughly pentagonal volcanic island located in the East Sea, approximately 130.3 km east of the Korean Peninsula, with a maximum elevation of 984 m above sea level. The exposed land mass area covers approximately 72 km^2 (11.3 km in length and 12.4 km in width) and supports approximately 10,800 inhabitants in 4500 households [31]. Most of the island has a complex topography that is very steep (Figure 2b), except for the Nari Basin to the north and residential areas. Most rock slopes along the coastal road are very steep (>55° inclination) and are weathered due to the environment exposed to close range of seawater. As such, rock slope failure and rock-fall problems occasionally happen [32]. The island is composed of volcanic rock such as basalt, trachyte, and andesite. The soil is very fertile and favorable for a clean water supply. Most of the land consists of forests, fields, and farmland. Ulleung Island has a seasonal oceanic climate (cool summer and warm winter), with an annual average temperature of 12 °C. There are numerous natural monuments and cultural assets designated by the provincial office and thus the island is known for its tourist attractions.

For the last decade, Ulleung Island has had an annual energy consumption of up to approximately 10,000 TOE (tonnage of oil equivalent), including petroleum, liquefied petroleum gas, electricity, and anthracite. The amount of electricity used reached 54,036 MWh in 2014 and electricity consumption is estimated to increase every year due to growing tourism [15]. The dominant source of electricity for several decades has been diesel generators. Problems associated with the use of diesel fuel have been its shipping cost from the mainland and environmental pollution. As mentioned above, therefore, the Korean government announced the plan to develop Ulleung Island into the green, low-carbon, energy-independent island with sustainable energy sources.

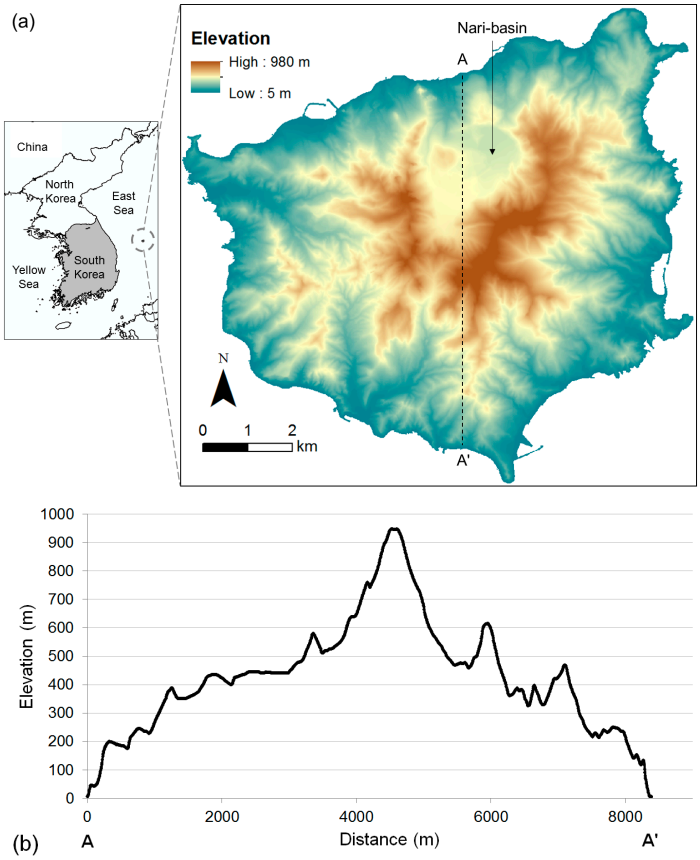

Figure 2. Study area: (**a**) geographical location and distributions of topography of Ulleung Island; and (**b**) vertical profile of A–A′ section showing very steep and complex topography (*x*-axis units span is approximately 5× that of the *y*-axis).

2.2. Identification of Constraint Variables

Table 2 lists eight constraint variables, their references, and the data source of the original data, selected based on a review of literature, local characteristics, and accessibility to the geo-referencing database. The areas and detailed explanation of each constraint factor layer can be identified in Figure A1 in Appendix A. Constraint variables in this case indicate conditions or areas where a PV solar energy development could not occur due to domestic protection laws and conservation regulations from the environmental, ecological, and engineering perspectives. Because PV systems have been recognized as a sustainable technology that can minimize the impact on local environments, areas such as environmental protection zones, ecological conservation zones, geo-technically high risk zones, and other limited development zones designated by local laws or regulations have been identified and removed from the selection process.

The eight vector-type constraint variables were spatially merged to generate a unified constraint polygon layer to create unified infeasible areas. This process makes it possible to create an output that combines all the characteristics of the input layers within one geographic area. The unified constraint polygon layer was then converted to a binary raster layer with a resolution of 5 m that has only values of 0 and 1. That is to say, a constraint raster layer was classified using a binary scale, where 0 represented the presence of a constraint and therefore was infeasible for development, and 1 represented the absence of a constraint and thus was potentially feasible for a development. The constraint layer will be used to exclude the constraint areas from each fuzzy index layer and final suitability layer.

Table 2. List of constraint variables and their referential rationale, original data extension, and data source of the original data. NSIC: National Spatial Information Clearinghouse of Korea; EGIS: Environmental Geographic Information Service of Korea; and WAMIS: Water Management Information System of Korea.

No.	Constraint Variable	Threshold	Reference	Data Source
C1	Residential areas	Itself	Regulation	NSIC
C2	Land use plan (urban, natural environment conservation areas)	Itself	Regulation	EGIS
C3	Tourist sites (historical areas, cultural heritage and archeological sites)	Itself	Regulation	EGIS
C4	Landscape designations (visual impact, scenic sites)	Itself	Regulation	EGIS
C5	Wildlife designations (birds protection zones, paleontological sites)	Itself	Regulation	EGIS
C6	Hydrographic areas (lakes, protection areas of source water, rivers, streams, water courses)	10 m buffer	Regulation	WAMIS
C7	Slope failure zone (rock fall)	10 m buffer	Local characteristics	Site investigation
C8	Elevation	>492 m	National low	NSIC

2.3. Identification of Factor Variables

Table 3 summarizes the six factor variables, their references, and the data source of the original data. The detailed explanation and the rationale of each factor variables and factor layer can be identified in Figure B1 in Appendix B. Selected factor variables should contain locale-specific characteristics that inform annual average power production and systems costs; e.g., local climate, meteorology, economics, and topography. Taking this into account, six factor variables were determined based on a review of literature, local characteristics, and accessibility to the geo-referencing database. The aspect (azimuth) of the landscape was not considered a dominant factor variable for this study, as ground-mounted PV systems may be installed facing the south on flat terrain or fairly steep slope areas where ground does not orient towards the south (For this reason, slope gradient factor variable was considered to identify flat terrain or gentle slope). This differs from rooftop-mounted PV systems.

Table 3. List of factor variables, original data extension, and data source of the original data. KMA: Korea Meteorological Administration; and KEPCO: Korea Electric Power Corporation.

No.	Factor Variable	Original File Extension	Data Source
F1	Solar irradiation ($kWh/m^2/day$)	Grid	Modeled using digital elevation model (DEM) and modified using KMA measured data (1 year for solar irradiation and average temperature, 20 years for sunshine hours)
F2	Equivalent sunshine hours (h)	Grid	
F3	Average temperature in summer (°C)	Point	
F4	3D path distance from nearest transmission line (m)	Polyline	Digitized and calculated from KEPCO data
F5	3D path distance from nearest road (m)	Polyline	Calculated from NSIC data
F6	Slope (°)	Grid	Calculated using DEM

All factor layers were extracted or generated to raster format with a grid cell of 5 m to keep uniformity with the unified constraint layer for the map algebraic analysis. A digital elevation model (DEM), which is a 3D representation of a surface of terrain with regularly gridded cells, was created

from contour data to be used as the basic data to derive the factor layer. Detailed data processing and the rationale for each factor layer were followed.

2.4. Application of Fuzzy Sets to Factor Variables

The factor variables each can have unique ranges, and thus each must be normalized for use within the MCE. Here, we apply a normalization method of FMFs. FMF enables to standardize the input raster into a 0 to 1 scale, indicating the strength of a membership in a data set, based on a specified fuzzification algorithm. To evaluate the degree of membership of a factor variable in a fuzzy set, numerous types of FMF have been developed and reported in the literature [33]. In Figure 3, we present the types of FMF used in this study. Determination of an FMF shape should be done with care, informed by physical constraints of the original data and the impact of these data on PV system performance and system costs, as the FMF shape can directly influence PV suitability. Here, all of the scaled factor variables contributed using an increasing or decreasing function based on the type of evidence and how each factor variable contributes to overall increased PV system performance and decreased system costs. The authors have sought out and removed conflicting evidence in function behavior and resulting performance changes.

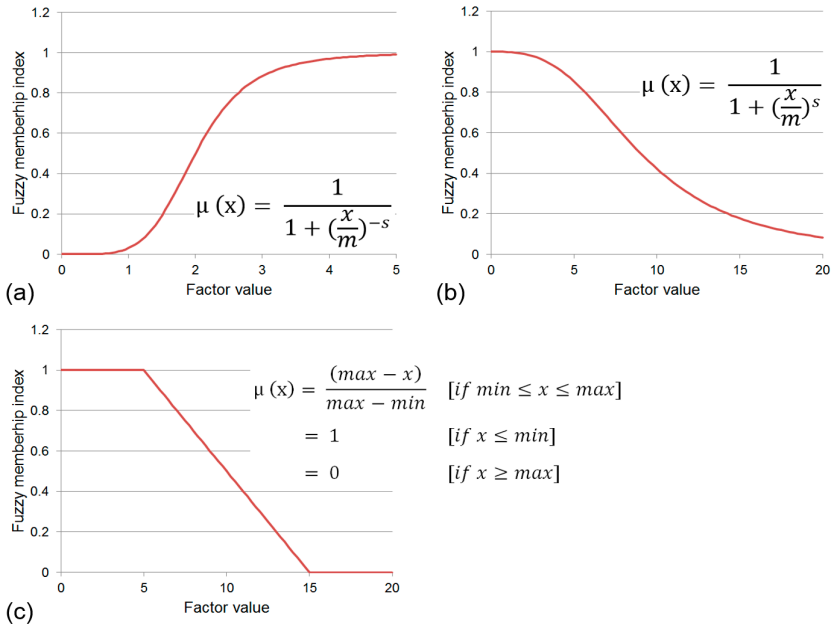

Figure 3. Types and forms of fuzzy membership functions used in this study: (**a**) fuzzy large (monotonically increasing function); (**b**) fuzzy small (monotonically decreasing function); and (**c**) fuzzy linear decreasing function (x: factor value, μ: fuzzy membership index, m: midpoint, s: spread, min: minimum factor value, max: maximum factor value).

The shape can be determined via the type of function, direction and its parameter settings as an FMF is a mathematical function. A monotonically increasing function (i.e., fuzzy large which makes a positive contribution seen in Figure 3a is useful when larger input values have a higher membership (higher PV suitability in this study). In contrast, a monotonically decreasing function (i.e., fuzzy small which makes a negative contribution seen in Figure 3b, fuzzy linear decreasing of Figure 3c) is used when smaller input values have a higher membership. Additional parameters depend on the type of selected function. For example, midpoint (m) and spread (s) parameters should be incorporated for fuzzy large and fuzzy small models whereas min and max parameters are required for fuzzy linear models. The defined midpoint identifies the crossover point (assigned a membership of 0.5). The spread parameter defines the shape of function by determining the degree of fuzzy membership

value change near midpoint. The larger the spread parameter value, the steeper the fuzzification around the midpoint. In other words, increasing the spread causes the fuzzy membership curve to become steeper. A fuzzy value of 1 means full membership in the specified fuzzy set (interpreted as the most suitable location for PV sites in this study), with membership decreasing to 0, indicating it is not a member of the fuzzy set (interpreted as not being a suitable location for PV sites).

The shape of FMF form for solar and climate factors (F1, F2, F3) was set to maximize electricity production capacity considering scientific relationships, such as correlations between the factor value and PV energy performance, whereas the shape of FMF form of proximity to infrastructure factors (F4, F5) and topography factors (F6) was set to minimize transmission losses and initial construction costs taking account of location-specific socio-economic conditions. In case we can only find a linearly decreasing relationship between a certain factor value and its PV suitability, Fuzzy Linear decreasing function opposed to Fuzzy Small function was adopted in this study. Detailed parameter values and their rationale were presented at the results section. Consequently, all the original factor values were normalized to a scale between 0 and 1. Thus far, each created fuzzy membership index layer continues to have equal importance if used to derive synthetic PV suitability.

2.5. Application of the Analytic Hierarchy Process Method to Factor Variables

The AHP technique, first suggested by Saaty [34], is an expert system that compares a number of variables by assigning a weight of importance relative to each factor variable being considered. Ten experts were solicited to assign a weight to each factor variable by completing a comparison matrix based on their experience, knowledge obtained from past research, or site investigations. Each expert contributor for this study (listed in the acknowledgments) has either worked in the field addressing solar PV energy site selection for several years or has pursued years of advanced research studies in the field of solar PV energy and/or site selection. The experts included a solar energy conversion system professional, PV potential assessment specialists, an energy economist, an urban designing professional, and experienced GIS analysts who had investigated study areas, and the second author who is a solar PV researcher and educator.

Pairwise comparison refers to the process of comparing several factors or elements in pairs to judge which factors is preferred (relative importance) or two factors are identically important in certain problem. Thus, it simplifying a complex problem and facilitating the determination of reasonable weights for multiple factors. In a pairwise comparison, the sum of weights of all criteria is 1. For example, in the case of four criteria (i.e., Factors A–D), a 4 × 4 matrix is required to determine the weights of the four criteria (Equation (1)).

$$\text{Matrix}: \begin{bmatrix} C_{11} & C_{12} & C_{13} & C_{14} \\ C_{21} & C_{22} & C_{23} & C_{24} \\ C_{31} & C_{32} & C_{33} & C_{34} \\ C_{41} & C_{42} & C_{43} & C_{44} \end{bmatrix} = \begin{bmatrix} 1 & C_{AB} & C_{AC} & C_{AD} \\ C_{BA} & 1 & C_{BC} & C_{BD} \\ C_{CA} & C_{CB} & 1 & C_{CD} \\ C_{DA} & C_{DB} & C_{DC} & 1 \end{bmatrix} \quad (1)$$

Each element of the pairwise comparison matrix indicates the value of the relative importance of the one factor to another factor, assigned using the intensity of importance scale of 1 to 9 [34] described in Table 4. For instance, if Factor *A* is much more important than Factor *B* in predicting a subsidence event, then a determined relative intensity value of 5 is assigned to C_{AB}. As the matrix is symmetrical, only the upper triangular half of the pairwise comparison matrix requires completion; the remaining elements are the reciprocals of the upper triangular half. The value of the diagonal elements of the matrix is 1.

Table 4. Fundamental scale for pairwise comparison to implement AHP technique (after Saaty [34]).

Intensity of Importance	Definition	Explanation
1	Equal importance	Two activities contribute equally to the objective
3	Moderate importance	Experience and judgment slightly favor one activity over another
5	Strong importance	Experience and judgment strongly favor one activity over another
7	Very strong or demonstrated importance	An activity is favored very strongly over another; its dominance demonstrated in practice
9	Extreme importance	The evidence favoring one activity over another is of the highest possible order of affirmation
2, 4, 6, 8	For compromise between the above values	Sometimes one needs to interpolate a compromise judgment numerically because there is no good word to describe it

When all element values of the pairwise comparison matrix were determined, a priority matrix, the normalized vector of the number of criteria, can be calculated according to:

$$P = \begin{bmatrix} p_1 \\ p_2 \\ p_3 \\ p_4 \end{bmatrix} = \begin{bmatrix} w_A \\ w_B \\ w_C \\ w_D \end{bmatrix} = \frac{1}{4} \times \begin{vmatrix} \sum_{j=1}^{4} \frac{c_{1j}}{c_{0j}} \\ \sum_{j=1}^{4} \frac{c_{2j}}{c_{0j}} \\ \sum_{j=1}^{4} \frac{c_{3j}}{c_{0j}} \\ \sum_{j=1}^{4} \frac{c_{4j}}{c_{0j}} \end{vmatrix} \quad \text{where } C_{0j} = \sum_{i=1}^{4} C_{ij} \tag{2}$$

where each element represents the weighting value of each criterion. The relative weight for each factor is determined within the range from 0 to 1; a higher weight indicates a greater contribution of the factor to PV suitability.

To identify the degree of consistency in assigning the values of elements in the pairwise comparison matrix, a consistency ratio (*CR*) can be used. The *CR* indicates the degree that participants' opinions are consistent in scoring of the pairwise comparison matrix and demonstrates the qualities of the causal factor of the PV suitability (in this case). The CR is defined as the ratio between the consistency index (*CI*) (Equation (4)) of the matrix and a random index (*RI*) shown in Equation (5). The RI can be assigned based on the number of criteria, using an appropriate value, as shown in Ishizaka and Labib [35]. In general, a *CR* value less than 0.1 is considered to indicate a valid comparison.

$$M = C \times P = \begin{bmatrix} m_1 \\ m_2 \\ m_3 \\ m_4 \end{bmatrix} \tag{3}$$

$$CI = \frac{\left(\frac{\sum_{i=1}^{4} \frac{m_i}{p_i}}{4} \right) - 4}{4 - 1} \tag{4}$$

$$CR = CI/RI \tag{5}$$

When the judgments of experts were different for a specific element of the comparison matrix, geometric mean values were used to combine preferences for each element to minimize the multiplicative error in calculating comparison matrix, as suggested in Ishizaka and Labib [35].

2.6. Identification of Suitability Index and Sensitivity Analysis

The PV solar farm *SI* was calculated for the entire grid of pixel digital numbers using a weighted sum method combining six fuzzy membership index layers with the weight of each factor being derived by the AHP technique (Equation (6)). The resulting cardinal scores for each alternative can be used to rank, screen, or choose an alternative [24]. Prior to aggregation of the six layers, each fuzzy membership index layer and the binary constraint layer were multiplied using the overlay method to exclude unified constraint areas from the suitability layer. This binary constraint layer behaves in a Boolean manner in the processing, to mask out areas from the model. A suitability map for the entire study area had the potential to have a maximum value of 1 (high suitability), and a minimum value of 0 (low suitability). This process makes it possible to create an integrated suitability layer that combines all the characteristics of the input layers within one geographic area.

$$\text{Suitability index} = \sum (\text{Fuzzy membership index}_i \times \text{Weight}_i) \quad (6)$$

where i indicates the i_{th} factor variable being considered.

Sensitivity analyses were carried out for two reasons. First, analyses were performed to assess the role of non-unique solutions for site selection given a defined set of criteria. In the process of developing this feasibility study, we considered the possibility for numerous cases to emerge that satisfied the criteria for optimal site selection. Under non-unique solution scenarios, the results would suggest the need for adaptation of the method via additional criteria and interpretations of the basic data to aid in decision-making strategies. For example, decision-makers may choose or change a plan to construct new energy infrastructure by considering additional criteria such as placement of future roads, building development, or planned transmission lines and power substations. The other reason is that the contribution of specific criteria (or factor variables) to suitability can vary according to electricity price, subsidy policy, and sector development. For example, as a sector develops and electricity prices go down with increased infrastructure, then climate criteria may become less important and location and environment criteria may become more so [18]. Therefore, four different *SI* were assessed by excluding the considered factor variables based on these scenarios: (Case 1) even weight for all factor variables; (Case 2) solar PV energy production factors only; (Case 3) natural environment factors only; (Case 4) all factors except slope factor. For each case, the remaining factor variables were kept in the same proportion to one another as produced by the weightings provided by the experts.

3. Results

3.1. Generation of a Unified Constraint Layer

The unified constraint areas are presented in Figure A2 in Appendix A. A grey region indicates the location of constraint areas and thus cannot be considered for a PV siting. The constraint region showed an area of approximately 44.2 km^2, which represents 60% of the study area. Most middle and eastern parts of study area were shown to be constraint areas predominantly because of tourist sites, landscape designations, and land use (or land use plans) such as urban areas and natural environment conservation areas. The figure also shows that non-constraint areas where PV siting is possible are located in relatively low-elevation regions.

3.2. Generation of Factor Layers

Six factor layers were generated from a variety of geospatial data using GIS-based spatial analysis (Figure B1 in Appendix B). The data showed that the average daily solar irradiation value ran from 0.2 kWh/m^2 to 3.7 kWh/m^2, the maximum daily sunshine hours was 5.5 h, and the average air temperature between 9 AM and 4 PM in summer was 20–27 °C. The maximum distance from the nearest transmission line and road were computed to be 2636 m and 1246 m, respectively. The slope layer

showed that Ulleung Island, being a volcanic island, is very mountainous with complex topography and a mean slope of approximately 32°.

3.3. Generation of Fuzzy Index Layers for Factor Variables

Table 5 summarizes the fuzzy membership functions, parameter values, and their references that were applied for each factor variable to rate the factor scores for the PV site selection in the study area. As this study is location-specific, it is inappropriate to directly adopt rating standards or scoring rules used in other studies where the study areas had different environments. To determine the shape of FMF suited for the characteristics of each factor, parameters were inputted based on their scientific basis, socio-economic conditions, local characteristics and local regulation. A detailed explanation of reasons for the assessment of conditions predisposed to high suitability expressed as a fuzzy index is given below.

Table 5. Applied fuzzy membership functions and the parameters and derived weight for each factor variable.

Factor	Fuzzy Function	Spread	Midpt	Minimum value	Maximum value	Reference	Weight
F1	Fuzzy Large	5	2	-	-	Min-Max value of Korea	0.3889
F2	Fuzzy Large	5	3.5	-	-	Min-Max value of Korea	0.2682
F3	Fuzzy Linear	-	-	27.3	20	Skoplaki and Palyvos [36]	0.0838
F4	Fuzzy Linear	-	-	3000	0	Local characteristics	0.1151
F5	Fuzzy Linear	-	-	1600	5	Local characteristics	0.0641
F6	Fuzzy Small	3	9	-	-	Local law and regulation	0.0799

Solar factor variables (F1, F2) were maximized since electricity production capacity increases with increasing solar factor values. Therefore, the Fuzzy Large function was applied for both factor layers. As parameters for two solar factors, a spread type of 5 with a shape similar to a sigmoidal model was selected and the midpoint was input taking into account the maximum value of observed data throughout Korea. For example, the maximum average annual solar irradiation value observed in the past 20 years in numerous cities in Korea was 3.93 kWh/m^2/day in Mokpo City [37]. Therefore, a solar irradiation value of 2 (approximately equal to half of 3.93) was set as the midpoint in this study. This allows the solar irradiation values of 0, 2, and 4 to be converted into fuzzy values of roughly 0, 0.5, and 1, respectively. For the equivalent sunshine hour factor, a value of 3.5 was set as the midpoint since the city with the longest annual sunshine duration in South Korea had an average daily sunshine of 6.26 h/day [38].

The climate factor variable (F3) requires specific temperature conditions to secure high power output since the cell efficiency and power output can change with varying temperature. In general, PV efficiency for power generation is linearly decreasing as the cell temperature is increasing [36]. The Fuzzy Linear function is useful if the membership is linearly decreasing at a specific value, so it was applied for this factor layer. The change of PV efficiency caused by changes in air temperature is frequently identified using nominal terrestrial environment (NTE) as a standard condition [36]. Based on the suggested air temperature condition of NTE, 20 °C was set as the min parameter for the maximum fuzzy index in the Fuzzy Linear model. A min and max parameter of 20 and 27.3 was input to the model respectively to define the appropriate decreasing zone taking into account linear correlation between PV efficiency and temperature.

The proximity to infrastructure factor variables (F4, F5) were minimized since PV sites with close grid connections or transport links are preferred due to lower potential investment costs. Therefore, the Fuzzy Linear decreasing function was applied for both factor variable layers. More specifically, proximity to transmission line can considerably reduce connection costs and/or transmission losses. A value of 0 was set as the max-parameter to be assigned a fuzzy index of 1 and 3000 was set as the min-parameter, with a fuzzy index of 0, taking into account the extent of study areas [20]. Proximity to transport links minimizes additional infrastructure construction and consequential damage to the

environment. For this factor variable, distance values of 4.5 and 1600 were set as the min and max parameter, respectively, considering the distribution of road lines in study areas. However, since it is not possible to build a PV plant on a road, the fuzzy index of road regions (4.5 m on either side of the center road line) were re-assigned as 0.

Topography factor variable (F6) was minimized since a PV plant requires flat terrain or a gentle slope because of access convenience [39]. Therefore, the Fuzzy Small function was applied to the slope factor layer. The local government recommends a slope limit value of 18° as a standard for PV solar farm infrastructure as well as large-scale construction in the study areas. Consequently, a value of 9 was set as the midpoint.

The six fuzzy membership index layers (one for each factor variable) that have been created are illustrated in Figure 4. The scale runs from 0 to 1 (or less) and higher fuzzy index indicates a better location for a PV plant. Areas with a high fuzzy index in Figure 4 coincide with the regions of high solar irradiation, longest sunshine hours, moderate air temperature, contiguousness to transmission lines, proximity to roads, and flatness of terrain.

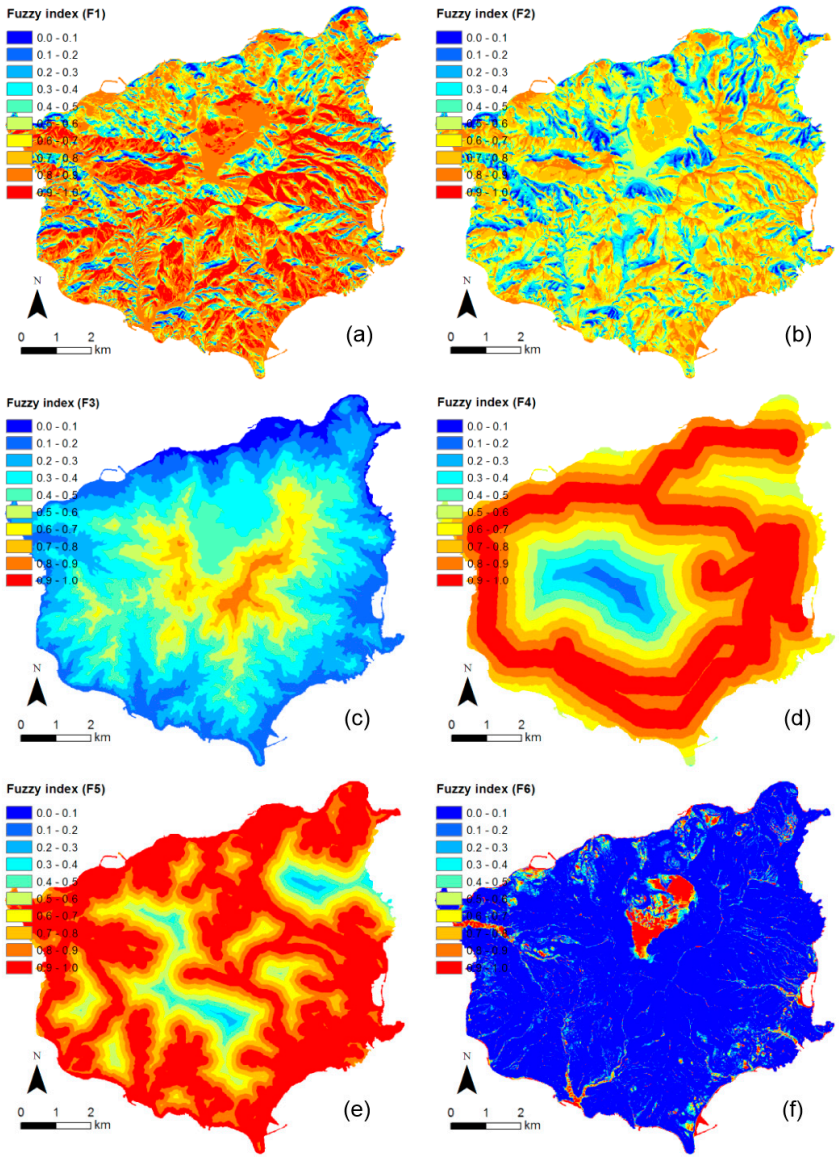

Figure 4. Fuzzy scaled inputs for each factor variable: (**a**) solar irradiation; (**b**) equivalent sunshine hours; (**c**) average temperature in summer; (**d**) 3D path distance from nearest transmission line; (**e**) 3D path distance from nearest road; and (**f**) slope.

3.4. Computation of Weightings of Each of the Factor Variables

The pairwise comparison completed by the experts indicated that solar irradiation showed the highest weight among all factors, followed by equivalent sunshine hours, proximity to transmission line, average daily temperature in summer, slope, and proximity to road (Table 5). In particular, the weightings significantly favored the solar factor variables (F1, F2), solar irradiation (0.3889) and equivalent sunshine hours (0.2682), since they are main sources of power production. This opinion seems to be similar to other published literature. In contrast, expert judgement indicated that the slope factor variable had a relatively high influence on PV siting compared with other previous studies [18,20]. This opinion stems from the fact that most regions of Ulleung Island are so rugged and steep that it is difficult to find flat terrain. The distance from nearest road factor variable did not carry much weight because the experts judged that the effect of this factor on the economic aspect would be low compared with the other factor variables considered.

From the values of the pairwise comparison matrix, the calculated CR in the present study was approximately 0.0144, which is an acceptable level of confidence (<0.1) for assigning weights to each factor variable. The weighting that was assigned using these results was utilized to aggregate fuzzy index.

3.5. Generation of Suitability Layers Using a Fuzzy-Analytic Hierarchy Process Integrated Model and Its Sensitivity Analysis

A suitability layer for a PV solar farm on Ulleung Island was generated by aggregating six weighted fuzzy membership indices based on Equation (6). Originally, the resulting map showed the *SI* to be between 0.09 and 0.92 (rounded off to two decimal places). This enables the ranking of areas in terms of the possibility of a PV plant relative to the scale and spatial extent of the study area. In other words, the computed *SI* does not represent an absolute possibility. Accordingly, the original map gives a visual interpretation of the seven classes of suitability: most extremely suitable ($SI > 0.85$) in red, extremely suitable (0.80–0.85) in orange, very strongly suitable (0.75–0.8) in yellow, strongly suitable (0.7–0.75) in green, moderately suitable (0.65–0.7) in sky-blue, marginally suitable (a capped value of 0.65) in blue, and constraint areas in grey (Figure 5).

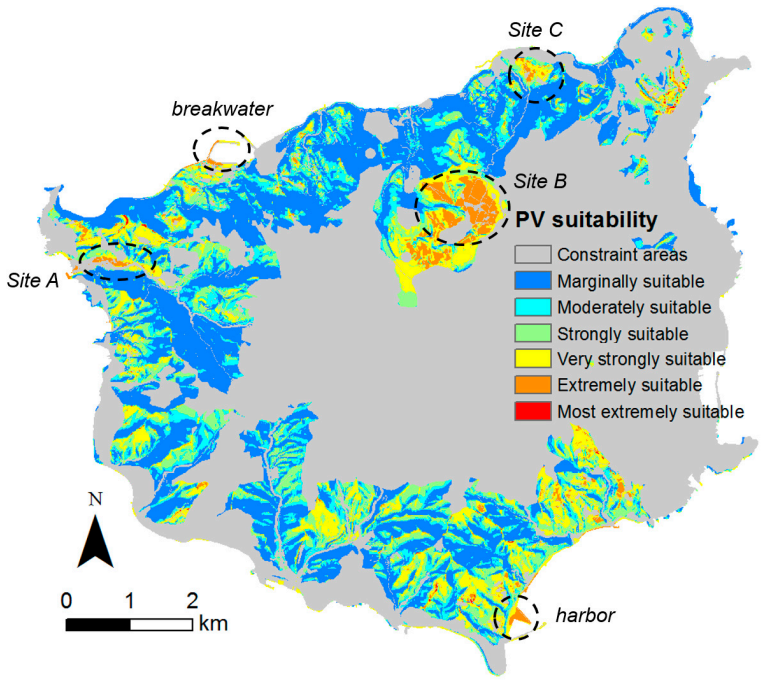

Figure 5. Suitability index (SI) for PV solar farm development on Ulleung Island.

The regions with an *SI* of more than 0.8 (in red and orange) accounted for approximately 1.6% of the study area. From these, three regions with wide aggregated neighboring extremely suitable areas were selected as candidate sites for a PV plant via the visual analysis presented in Figure 5 and were named Site A (western part), Site B (middle part), and Site C (northern part).

The average values of each of the factor values within the three sites were analyzed using zonal statistics (Table 6). We determined that all three sites have characteristics in common in terms of solar irradiation, proximity to infrastructure, and slope conditions. Specifically, they were located in areas of moderate to high daily insolation (2.91–3.04 kWh/m^2/day) but not in the regions of the highest solar irradiation in the study area. Furthermore, these three sites coincide with locations of existing transmission lines (139–332 m) and roads (<58 m); however, we could not make a clear difference between proximity to roads between the most extremely suitable region and the rest of the five suitable regions. Most of these three sites showed a slope condition that had a gentle slope and this was the distinct difference between "extremely suitable" ($SI > 0.8$) or the remaining five suitable regions and other suitable ($SI \leq 0.8$) regions. In particular, Site B showed a larger area (0.61 km^2) compared with that of Site A and C. In case of Site B, solar irradiation values were relatively high compared with that of Site A and C, although the sunshine hour factor showed relatively low values.

Table 6. Statistical summary of average factor variable values and the areas within the three candidate sites.

Factor Variable	Site A	Site B	Site C
Solar irradiation (kWh/m^2/day)	2.91	3.04	2.99
Equivalent sunshine hours (h)	4.57	4.33	4.90
Average temperature in summer (°C)	25.96	24.70	26.57
3D path distance from nearest transmission line (m)	139.76	332.53	202.32
3D path distance from nearest road (m)	18.15	57.88	34.31
Slope (°)	3.15	2.68	2.45
Area (km^2)	0.04	0.61	0.03

The area for PV installation necessary to produce all the electricity needed on the study area was calculated with simplified, conservative assumptions (annual energy consumption: 54,036 MWh/year, PV module capacity: 1000 kWh/kWp/year each, Area per unit module: 6 m^2/kWp, and Area ratio coefficient between module area and land area to account for distance between module racks to avoid shadowing: 2.5). As a result, it was estimated that an area of approximately 0.81 km^2 (1.34× the area of Site B) would be called for to generate electricity solely with a centralized PV system on Ulleung Island. While the Green Ulleung Island project will consider all the possible other renewable energy sources, this survey result for Sites A–C supports the role of PVs as a strong option.

In the sensitivity analysis, the factor variables that were considered were excluded in the *SI* calculation process to obtain four different results. Figure 6 presents four suitability layers, expressed on a scale with seven classes based on four scenarios. In Case 1 (Figure 6a), the weightings of all factors were equally changed to 1 to examine the result of a non-weighted fuzzy index summation. As a result, extremely suitable regions with an *SI* of more than 0.8 in orange decreased, including Site B. In Case 2 (Figure 6b), only solar and climate factors (F1, F2, and F3) were considered in order to identify the most suitable areas only in terms of electricity production. As a result, the area of regions extremely suitable for PV plants was increased compared with the original results. In Case 3 (Figure 6c), proximity to infrastructure factors (F4, F5) was excluded in the calculation to reflect only natural environmental factors. This can provide a meaningful result since this exclusion will allow the identification of potential pathways for future transmission lines or road development to pass near extremely suitable locations for synthetic renewable energy developments for a green island as well as PV plant implementations. Due to the aforementioned reason that most of infrastructure exists on most areas of the six-class suitable regions, however, there was no visible difference from

the original result. In Case 4 (Figure 6d), the slope factor (F6) was excluded when assessing the SI. Consequently, the regions which were extremely suitable for PV plants were much more extensive over entire areas than in the original results. This layer will be useful when the PV project has enough economic feasibility taking into account land clearing and site construction costs.

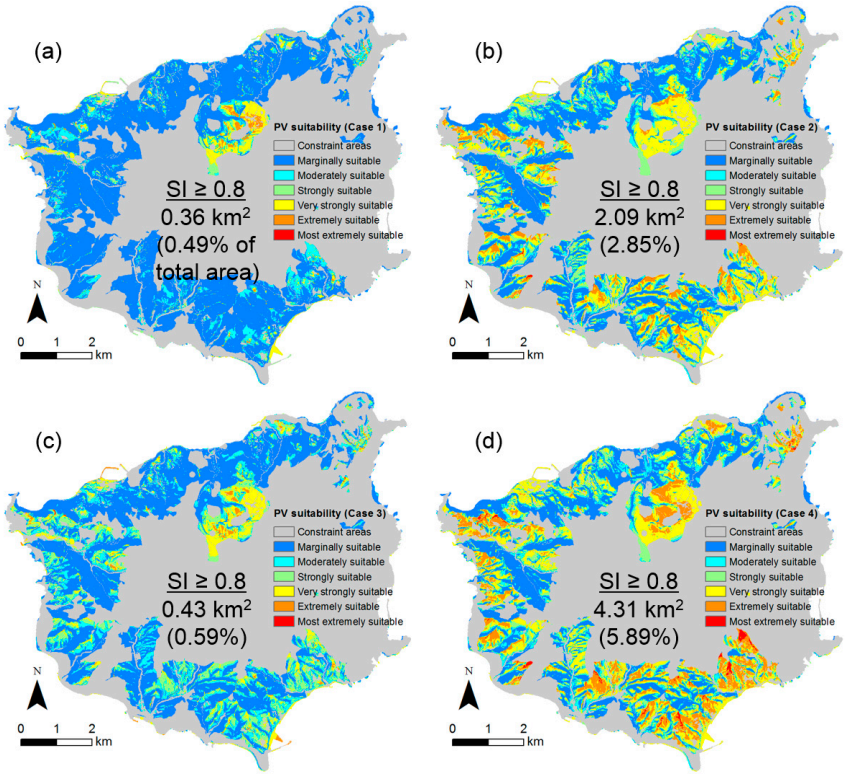

Figure 6. Sensitivity analysis of the *SI* results for PV solar farm development: (**a**) Case 1: Even weight for all factor variables; (**b**) Case 2: Only solar PV energy production factors (solar irradiation, sunshine hours, average daily temperature in summer); (**c**) Case 3: Only natural environmental factors (excluding proximity to grid connection and proximity to road) and (**d**) Case 4: All factors except slope factor.

4. Discussion

4.1. Validation of the Model

Although the suitability layer above showed four regions with most extremely or extremely suitable classes, they are only results based on the MCE model designed in this study. In other words, validation for the resulting map is required to determine whether the aforementioned three sites are really the most suitable or not. Therefore, a validation process was applied to identify whether the grid cells showing the extremely suitable zones at a certain set of coordinates are actually areas that are appropriate for PV sites in the real world. The representative extremely suitable zones and corresponding Google Earth satellite images are shown in Figure 7. From the high-resolution satellite images, it can be seen that most of the area in the three sites consist of grassland or agricultural areas. This indicates that the aforementioned three sites on the resulting maps can be used as PV plants in the real world. However, a building was found on the west side region of Site C (northern part), and it should be removed at the most extremely suitable areas. Southern part of Figure 5 was observed to be the most extremely suitable region but an inappropriate region for a PV site in the real world because it is a harbor area. These examples show that these kinds of small-sized infrastructure or buildings should be regarded as some level of constraint and checked in the final phase of a detailed ground site investigation.

No large-scale PV solar farm exists yet on Ulleung Island, although there are small-scale PV systems (≤3 kWp each) or rooftop PV developments which were not designed with scientific investigations [15]. As such, the map results obtained from this study cannot be validated with existing PV solar farms on Ulleung Island.

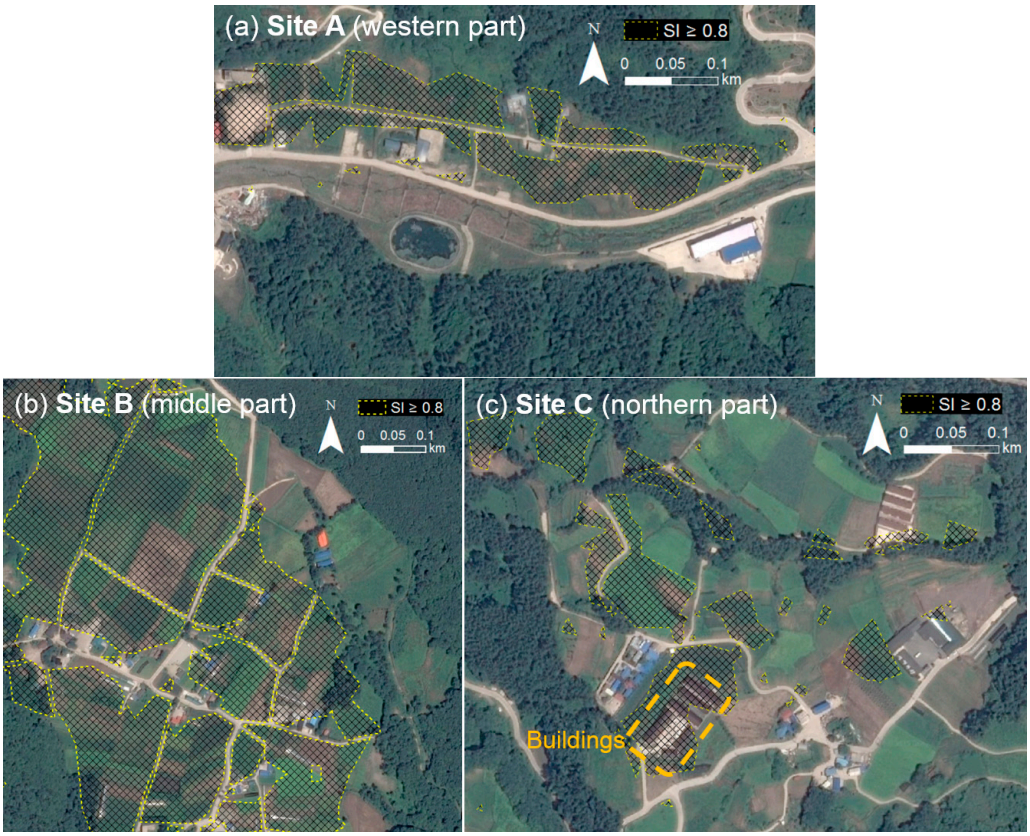

Figure 7. Satellite images (source from: Google Earth, http://www.google.com/earth/index.html) of each part of three candidate areas for the validation of the map results: (**a**) Site A: western part; (**b**) Site B: middle part and (**c**) Site C: northern part.

4.2. Location-Specific Slope Condition

The environment of the study areas is intensively different from that of similar studies because this is a volcanic island with complex topography. Consequently, contrary to what has been found in previously published literature, slope was a key screening factor in defining the three candidate sites from the five-class suitable zones in this study. The slope of Ulleung Island showed range of 0°–83° while 0°–50° is the range used in other PV siting studies [25]. In addition, most previous studies [19,22] proposed a constraint threshold for the slope to be a range of 5°–10°. In the case of Ulleung Island, only 3.42 km^2 (5% of total area) has a gently steep terrain of 5° or less gradient and only 6.01 km^2 (9%) is 10° or less. These percentage numbers are considerably lower than those found in other studies above. As such, stakeholders or decision makers have to consider other PV systems such as building rooftops or street lamps as supplements. In the same way that the slope threshold in other studies does not apply to Ulleung Island, the one used in this study is not directly usable in other island cases with different topographic characteristics.

5. Conclusions

This study suggested an adaptive MCE-based method to identify suitable areas for centralized solar PV arrays based on practitioner-informed criteria for a given locale. Here, we have demonstrated

the method to find three highly suitable regions within the constrained area of Ulleung Island using a weighted fuzzy summation method within a GIS environment. The results obtained from this study can potentially contribute to reductions in levelized costs of electricity (LCOE) for regional siting of solar farms by favoring factor variables that offer the highest values for solar power conversion (high solar irradiation, longest sunshine hours, and low average air temperature) and lowest cost criteria for BoS (by proximity to existing transmission lines and roads) for PV installations. Furthermore, this work indicates that the criteria for suitability can be adapted by local practitioners to be used as a planning method to minimize the impact on the environment, society, and infrastructure when converting from fossil fuel combustion to green infrastructure. In this particular study, our approach may aid decision makers in moving towards a desired goal of having more than 90% of Ulleung Island's electricity generated by renewable energy resources, including PV, by 2030.

Nevertheless, there are ways to improve the analysis process for this locale in future work. The present irradiance data are highly simplified, yet they enable to screen or narrow the appropriate areas for PV system of the large area of the island. Using the preliminary assessment method here, one can envisage community planners recommending investments in local ground monitoring stations for the three sites based on solar irradiance data collected on the identified sites over years, for feasibility and due diligence steps of solar project development [40]. Better decisions can also be made by taking into account evolving economic considerations, such as the shifts in public price of land and costs for land clearing and construction. As with solar monitoring, extensive field surveys must follow for PV candidate sites in order to identify and validate locally important constraint and factor variables from the urban planning perspective. In addition, shared analyses of other available low-carbon energy alternatives can be coupled with a solar siting study, to enable regional planning for renewable energy diversity in the future.

These findings may be applicable to other areas lacking grid connectivity, as the method used is highly adaptive, and may be applied to other areas, such as rural West Africa and India with appropriate informed local practitioner criteria that takes into account locale-specific variables. With these adaptations, the suggested GIS-based suitability assessment model can be used as an informative and enabling site selection tool for screening optimal PV sites in other areas of the world.

Acknowledgments: The authors would like to thank participating experts, Yosoon Choi, Youah Lee, Joohyun Cho, Heechul Kim, Sangho Lee, Sungmin Kim, Mesude Bayrakci, Vivek Srikrishnan, Jinyoung Song, Myungchan Oh, who completed the pairwise comparison matrix of AHP work. The authors thank anonymous reviewers for their critical comments and suggestions, which greatly improved the quality of our manuscript.

Author Contributions: Jangwon Suh designed the research and analyzed all the GIS data; Jangwon Suh and Jeffrey R.S. Brownson interpreted the results and wrote the paper.

Conflicts of Interest: The authors declare no conflict of interest.

Abbreviations

MCE	Multi-criteria evaluation
GIS	Geographic information system
PV	Photovoltaics
SI	Suitability index
BoS	Balance of system
MCDA	Multi-criteria decision analysis
AHP	Analytic hierarchy process
FLOWA	Fuzzy logic ordered weight averaging
DEM	Digital elevation model
FMF	Fuzzy membership functions
CR	Consistency ratio
RI	Random index
NTE	Nominal terrestrial environment
KMA	Korea meteorological administration

Appendix A. Maps Used for Constraint Variables

(C1) Residential areas: This layer was extracted from a land cover map, provided by National Spatial Information Clearinghouse (NSIC) of South Korea, which consists of coniferous forests, arid ground, dry field, residential areas (Code 4), bare ground, roads, and grassland. Residential areas are one of the most frequently used constraint variables in PV site selection analyses.

(C2) Land use plan: Urban (Code 4) and natural environment conservation areas (Code 3) were extracted from a land use map, provided by Environmental Geographic Information Service (EGIS) of South Korea, which consists of four different classifications. Natural environment conservation areas included some parts of tourist sites, landscape designations, and wildlife designations.

(C3) Tourist sites: This layer is composed of historical areas and cultural heritage and archeological sites. It was extracted from separate management areas of an ecological zoning map which represents four different grades (Grades 1–3, and separate management areas) for the natural environment based on its ecological value, landscape value, and other aspects.

(C4) Landscape designations: This layer is composed of regions associated with visual impact and scenic sites. It also was extracted using the same data sources as the tourist sites. These areas were excluded from PV sites due to environmental protection and ecological conservation.

(C5) Wildlife designations: This layer is composed of bird protection zones and paleontological sites. It was extracted from Grade 1 (region and topography) of an ecological zoning map for the conservation and restoration of the natural environment established by regulation. Buffering analysis was not considered due to the fact that PV development is environmentally benign.

(C6) Hydrographic areas: This layer is composed of lakes, protection areas of source water, rivers, streams, and water courses. It was extracted from hydrographic and hydrogeological map. Ten-meter buffering analysis was applied to polyline-type layers (river, streams, and water courses) to represent their width.

(C7) Slope failure zone: This layer was created from a geological site investigation for rock slope failures including rock falls along the coast roads. Ten-meter buffering analysis was applied to surveyed points considering their influence areas (geo-hazard zone). It should be noted that slope failure is only specific to the region and may not apply to other regions.

(C8) Elevation: This layer was extracted from a DEM which shows a 3D representation of a surface of the terrain with a regularly gridded cell. The regions above 492 m (50% of maximum elevation) were regarded as constraint regions based on the national law that building a large-scale infrastructure in those regions is not permitted.

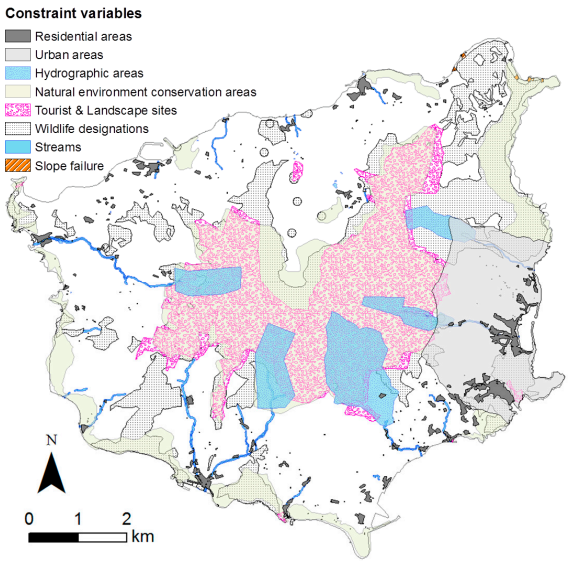

Figure A1. Distributions of constraint areas used in this study.

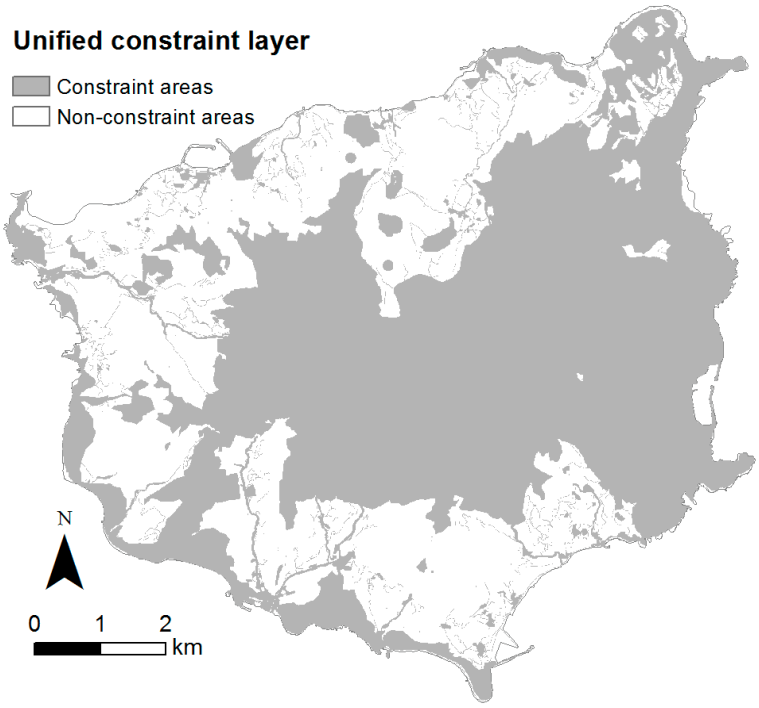

Figure A2. Unified binary constraint layer showing areas forbidden to PV farm development.

Appendix B. Maps Used for Each Factor Variable

(F1) Solar irradiation: This indicates the incident shortwave energy per unit area. Solar irradiation can affect average annual power performance and thus is regarded as one of the most important factors in PV suitability analysis. Hence, the most isolated areas are predisposed to high PV suitability. Two years of officially observed solar irradiation hourly data for Ulleung Island are available for a few points. However, it is not possible in practice to predict or generate solar irradiation values for the entire grid of cells of the study areas with limited observed data as solar irradiation can be easily affected by or vary due to neighboring topographic environments. Therefore, solar irradiance values were calculated by the summation of direct and diffuse irradiation for the entire grid of cells using DEM data (raster surface) and ArcMap solar irradiation tools based on methods from the hemispherical viewshed algorithm [41]. These tools can roughly estimate a simplified average annual solar irradiation condition (much like one can estimate average annual temperatures) over the grid cells considering shading effect of neighboring topographic environment and have been frequently used in regional or national-scale PV potential assessment and solar farm site selection studies [19,22,42–45]. It should be noted, in reality, the calculation of the annual average irradiation will depend quite strongly on how the typical weather is in the different seasons. Latitude was set to 37.5° decimal degrees in modeling. A shortwave transmissivity value of $\tau = 0.45$ was input as no published literature on that value of the study area was available. Subsequently, modeled solar irradiation values were modified using their correlation with data observed at several points (Automated Synoptic Observing System (ASOS) and Automated Weather Station (AWS)) in 2010 by the Korea meteorological administration (KMA). This is reasonable because modification by observed data can decrease the uncertainty of a parameter (atmospheric transmissivity) input to modeled data.

(F2) Equivalent sunshine hours: This represents the duration (in hours) of direct solar irradiation that exceeds a direct normal irradiance (DNI) of 120 W/m^2. Sunshine hours, one of the most frequently used factors in PV site selection research, is closely associated with amount of electricity production. For a reason similar to the one mentioned above, sunshine hours was calculated from DEM data using solar radiation tools of ArcMap software. Since these tools can identify non-shaded areas based on local topography and location of sun but not accurate meteorology, the calculated values were

then modified using a regression equation between modeled sunshine hours and average observed sunshine hours data at a few points for the past 20 years from the KMA. This makes sense as two different data areas can be used to complement each other in compiling the sunshine hours layer. F1 and F2 factor values can be correlated in a certain place, though they may not according to the topographical environment of study area.

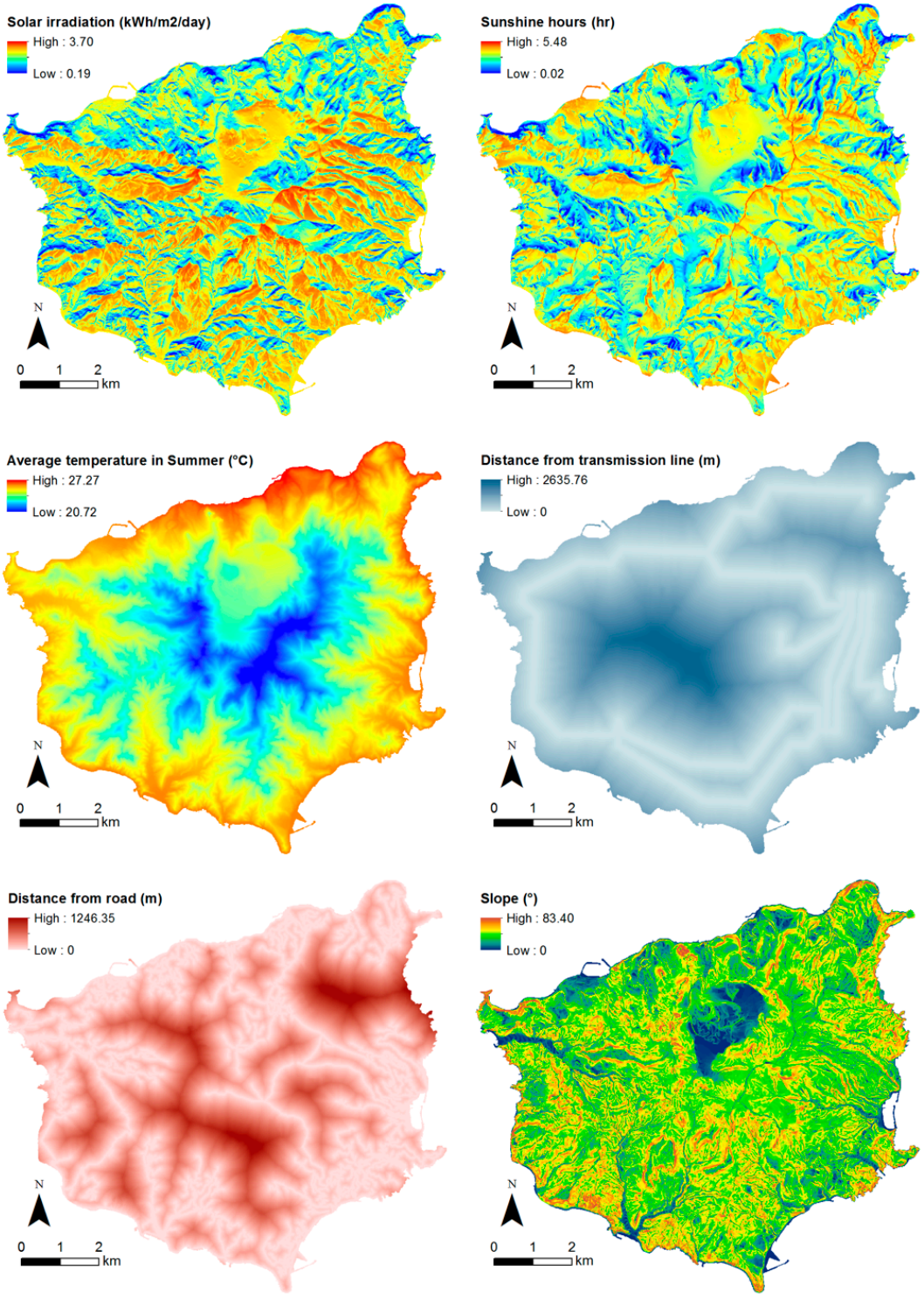

Figure B1. Factor layers which enable selective project goals used in this study.

(F3) Average daily temperature in summer: This refers to the average daily temperature from 9 AM to 4 PM in summer (between summer solstice and autumnal equinox day). Most silicon-based PV cells or modules' electrical efficiency is dependent on the cell temperature, which can be affected by terrestrial environment factors such as irradiance, ambient temperature, wind speed, mounting method, and material parameters [36]. In particular, a rise in the PV cell temperature causes a decrease in the voltage and a slight increase in the electric current. The temperature also affects some parameters such as minority carrier lifetime, carrier mobility, and diffusion and increases recombination in solar cells [46]. As such, given similar irradiation conditions, higher PV cell temperatures can lead to decreases in efficiency of power generation. This is why this variable was chosen for this study. Average daily temperature was obtained from the KMA data observed between 9 AM to 4 PM (the approximate duration for generating electricity) for 94 days in the summer of 2010 to keep uniformity with the observation period (year) of the solar irradiation. It is found that the average daily temperature for other seasons (during autumnal equinox day and summer solstice) showed below the 20 °C appropriate for generating electricity.

(F4) 3D path distance from nearest transmission line: This indicates surface length, both horizontal and vertical distance simultaneously, between a grid cell and nearest existing transmission line. Proximity to transmission lines is one of the most commonly considered factors relevant to the potential investment costs. As Ulleung Island has complex topography, 2D Euclidean distance will be inaccurate when there is a surface that vertically varies greatly. Accordingly, the path distance module was applied to digitized existing transmission line data to generate 3D surface length from the nearest transmission line layer.

(F5) 3D path distance from nearest road: This represents 3D distance between a grid cell and the nearest existing roads. Similar to the above, proximity to roads is also associated with the BoS cost. Distance from the nearest road layer was generated applying the concept of 3D distance along the surface in this study.

(F6) Slope: This refers to the degree of topographic incline calculated as the maximum rate of change between a given cell center and that of its immediate neighbors. Slope, one of the important factors used for site selection research, is tied up with the pre-construction project costs. Slope was derived from DEM data using the surface analysis module.

References

1. Edenhofer, O.; Pichs-Madruga, R.; Sokona, Y.; Farahani, E.; Kadner, S.; Seyboth, K.; Adler, A.; Baum, I.; Brunner, S.; Eickemeier, P.; et al. *Climate Change 2014: Mitigation of Climate Change*; Intergovernmental Panel on Climate Change (IPCC): Cambridge, UK; New York, NY, USA, 2014.
2. United Nations Climate Change Conference (COP 21). Available online: http://www.cop21.gouv.fr/en/195-countries-adopt-the-first-universal-climate-agreement (accessed on 7 January 2016).
3. Uemura, Y.; Kai, T.; Natori, R.; Takahashi, T.; Hatate, Y.; Yoshida, M. Potential of renewable energy sources and its applications in Yakushima Island. *Renew. Energy* **2004**, *29*, 581–591. [CrossRef]
4. Demiroren, A.; Yilmaz, U. Analysis of change in electric energy cost with using renewable energy sources in Gökceada, Turkey: An island example. *Renew. Sustain. Energy Rev.* **2010**, *14*, 323–333. [CrossRef]
5. Liu, H.-Y.; Wu, S.-D. An assessment on the planning and construction of an island renewable energy system –A case study of Kinmen Island. *Renew. Energy* **2010**, *35*, 2723–2731. [CrossRef]
6. Trappey, A.J.C.; Trappey, C.V.; Lin, G.Y.P.; Chang, Y.-S. The analysis of renewable energy policies for the Taiwan Penghu island administrative region. *Renew. Sustain. Energy Rev.* **2012**, *16*, 958–965. [CrossRef]
7. Sakaguchi, T.; Tabata, T. 100% electric power potential of PV, wind power, and biomass energy in Awaji island Japan. *Renew. Sustain. Energy Rev.* **2015**, *51*, 1156–1165. [CrossRef]
8. Mosey, G.; Heimiller, D.; Dahle, D.; Vimmerstedt, L.; Brady-Sabeff, L. *Converting Limbo Lands to Energy-Generating Stations: Renewable Energy Technologies on Underused, Formerly Contaminated Sites*; National Renewable Energy Laboratory: Golden, CO, USA, 2007.
9. Song, J.; Choi, Y. Design of photovoltaic systems to power aerators for natural purification of acid mine drainage. *Renew. Energy* **2015**, *83*, 759–766. [CrossRef]

10. Song, J.; Choi, Y. Analysis of the Potential for Use of Floating Photovoltaic Systems on Mine Pit Lakes: Case Study at the Ssangyong Open-Pit Limestone Mine in Korea. *Energies* **2016**, *9*, 102. [CrossRef]
11. Brownson, J.R.S. *Solar Energy Conversion Systems*, 1st ed.; Elsevier-Academic Press: Oxford, UK, 2014; pp. 237–251.
12. Dincer, I. Environmental impacts of energy. *Energy Policy* **1999**, *27*, 845–854. [CrossRef]
13. Akella, A.K.; Saini, R.P.; Sharma, M.P. Social, economical and environmental impacts of renewable energy systems. *Renew. Energy* **2009**, *34*, 390–396. [CrossRef]
14. DGI. *Ulleung and Dokdo Island: Korea's Sustainable Energy Island Project*; Daegu Gyoengbuk Development Institute: Daegu, Korea, 2010.
15. MKE. *The Study on Comprehensive Plan for Constructing Ulleung Sustainable Energy Island*; The Ministry of Knowledge Economy of Korea: Seoul, Korea, 2012.
16. MKE. *A Preliminary Study on a Demonstration of Green City*; The Ministry of Knowledge Economy of Korea: Seoul, Korea, 2009.
17. Environmental Protection Agency (EPA). Available online: https://www.epa.gov/re-powering (accessed on 15 August 2016).
18. Carrión, J.A.; Estrella, A.E.; Dols, F.A.; Toro, M.Z.; Rodríguez, M.; Ridao, A.R. Environmental decision-support systems for evaluating the carrying capacity of land areas: Optimal site selection for grid-connected photovoltaic power plants. *Renew. Sustain. Energy Rev.* **2008**, *12*, 2358–2380. [CrossRef]
19. Charabi, Y.; Gastli, A. PV site suitability analysis using GIS-based spatial fuzzy multi-criteria evaluation. *Renew. Energy* **2011**, *36*, 2554–2561. [CrossRef]
20. Uyan, M. GIS-based solar farms site selection using analytic hierarchy process (AHP) in Karapinar region, Konya/Turkey. *Renew. Sustain. Energy Rev.* **2013**, *28*, 11–17. [CrossRef]
21. Sánchez-Lozano, J.M.; Henggeler Antunes, C.; García-Cascales, M.S.; Dias, L.C. GIS-based photovoltaic solar farms site selection using ELECTRE-TRI: Evaluating the case for Torre Pacheco, Murcia, Southeast of Spain. *Renew. Energy* **2014**, *66*, 478–494. [CrossRef]
22. Watson, J.J.W.; Hudson, M.D. Regional Scale wind farm and solar farm suitability assessment using GIS-assisted multi-criteria evaluation. *Landsc. Urban Plan.* **2015**, *138*, 20–31. [CrossRef]
23. Pohekar, S.D.; Ramachandran, M. Application of multi-criteria decision making to sustainable energy planning—A review. *Renew. Sustain. Energy Rev.* **2004**, *8*, 365–381. [CrossRef]
24. Wang, J.-J.; Jing, Y.-Y.; Zhang, C.-F.; Zhao, J.-H. Review on multi-criteria decision analysis aid in sustainable energy decision-making. *Renew. Sustain. Energy Rev.* **2009**, *13*, 2263–2278. [CrossRef]
25. Sánchez-Lozano, J.M.; Teruel-Solano, J.; Soto-Elvira, P.L.; Socorro García-Cascales, M. Geographical Information Systems (GIS) and Multi-Criteria Decision Making (MCDM) methods for the evaluation of solar farms locations: Case study in south-eastern Spain. *Renew. Sustain. Energy Rev.* **2013**, *24*, 544–556. [CrossRef]
26. Zadeh, L.A. Fuzzy sets. *Inf. Control* **1965**, *8*, 338–353. [CrossRef]
27. Droj, G. Increasing Classification Quality by Using Fuzzy Logic. *J. Appl. Eng. Sci.* **2011**, *1*, 61–66.
28. Carver, S.J. Integrating multi-criteria evaluation with geographical information systems. *Int. J. Geogr. Inf. Syst.* **1991**, *5*, 321–339. [CrossRef]
29. Jankowiski, P. Integrating geographical information systems and multiple criteria decision-making methods. *Int. J. Geogr. Inf. Syst.* **1995**, *9*, 251–273. [CrossRef]
30. Malczewski, J. GIS-based multicriteria decision analysis: A survey of the literature. *Int. J. Geogr. Inf. Sci.* **2006**, *20*, 703–726. [CrossRef]
31. Local Information of Ulleung Island. Available online: http://www.ulleung.go.kr/English (accessed on 30 November 2015).
32. Lee, S.; Suh, J.; Park, H.D. Smart Compass-Clinometer: A smartphone application for easy and rapid geological site investigation. *Comput. Geosci.* **2013**, *61*, 32–42. [CrossRef]
33. Robinson, V.B. A Perspective on the Fundamentals of Fuzzy Sets and their Use in Geographic Information Systems. *Trans. GIS* **2003**, *7*, 3–30. [CrossRef]
34. Saaty, T.L. A scaling methods for priorities in hierarchical structures. *J. Math. Psychol.* **1977**, *15*, 234–281. [CrossRef]
35. Ishizaka, A.; Labib, A. Review of the main developments in the analytic hierarchy process. *Expert Syst. Appl.* **2011**, *38*, 14336–14345. [CrossRef]

36. Skoplaki, E.; Palyvos, J.A. On the temperature dependence of photovoltaic module electrical performance: A review of efficiency/power correlations. *Sol. Energy* **2009**, *83*, 614–624. [CrossRef]
37. Korea Meteorological Administration (KMA). Available online: http://www.kma.go.kr/weather/climate/solar_energy01.jsp?type=1&element=10&year=2010&x=26&y=7 (accessed on 30 November 2015).
38. Korea Meteorological Administration (KMA). Available online: http://www.kma.go.kr/weather/climate/solar_energy01.jsp?type=1&element=9&year=2010&x=21&y=11 (accessed on 30 November 2015).
39. Korea Law Information Systems. Available online: http://www.law.go.kr (accessed on 30 November 2015).
40. Sengupta, M.; Habte, A.; Kurtz, S.; Dobos, A.; Wilbert, S.; Lorenz, E.; Stoffel, T.; Renné, D.; Gueymard, C.; Myers, D.; et al. *Best Practices Handbook for the Collection and Use of Solar Resource Data for Solar Energy Applications*; Technical Report NREL/TP-5D00-63112; National Renewable Energy Laboratory: Denver, CO, USA, 2015.
41. Fu, P.; Rich, P. A geometric solar radiation model with applications in agriculture and forestry. *Comput. Electron. Agric.* **2002**, *37*, 25–35. [CrossRef]
42. Gastli, A.; Charabi, Y.; Zekri, S. GIS-based assessment of combined CSP electric power and seawater desalination plant for Duqum—Oman. *Renew. Sustain. Energy Rev.* **2010**, *14*, 821–827. [CrossRef]
43. Gastli, A.; Charabi, Y. Solar electricity prospects in Oman using GIS-based solar radiation maps. *Renew. Sustain. Energy Rev.* **2010**, *14*, 790–797. [CrossRef]
44. Brito, M.C.; Gomes, N.; Santos, T.; Tenedório, J.A. Photovoltaic potential in a Lisbon suburb using LiDAR data. *Sol. Energy* **2012**, *86*, 283–288. [CrossRef]
45. Bayrakci Boz, M.; Calvert, K.; Brownson, J.R.S. An automated model for rooftop PV systems assessment in ArcGIS using LIDAR. *AIMS Energy* **2015**, *3*, 401–420. [CrossRef]
46. Bayrakci, M.; Choi, Y.; Brownson, J.R.S. Temperature Dependent Power Modeling of Photovoltaics. *Energy Procedia* **2014**, *57*, 745–754. [CrossRef]